Workshop on Nuclear Matter in Different Phases and Transitions *LBNL-41824*
Centre de Physique, Les Houches, France *March 31 - April 10, 1998*

DYNAMICS OF THE CHIRAL PHASE TRANSITION

JØRGEN RANDRUP
Nuclear Science Division, Lawrence Berkeley Laboratory
Berkeley, California 94720, USA

1. Introduction

The advent of ever more powerful heavy-ion accelerators has made it possible to study nuclear matter in different phases and transitions. In particular, at the unprecedented energy densities now within reach at RHIC, two fundamental phase changes are expected to occur. One is the dissolution of ordinary hadrons into a deconfined quark-gluon plasma phase, which has long been a principal research objective. The other, with which the present discussion concerned, is the approximate restoration of chiral symmetry. This topic has gained increasing interest in recent years, especially because of the possibility of forming *disoriented chiral condensates*, the agitation of coherent oscillations of the pion field as a result of the rapid non-equilibrium dynamics. Reviews are given in refs. [1, 2, 3].

Since the quark masses are fairly small, the basic QCD Lagrangian is approximately invariant with respect to chiral transformations. However, due to the self-interaction of the fields, this symmetry is spontaneously broken by the vaccum, leading to a finite value of the order parameter, $<q\bar{q}> = f_\pi$. Furthermore, the associated pionic excitations are approximately massless on the hadronic scale. This basic feature of the strong interaction may be probed in high-energy collisions of hadrons or nuclei as follows. The early violent part of a collision event produces an extended region of space within which the energy density is so high that chiral symmetry is temporarily nearly restored. As the collision evolves further, the energy density drops so rapidly that the chiral degrees of freedom fall out of equilibrium, leading to large-amplitude long-wavelength isospin-directed oscillations of the pion field. This unique phenomenon would have a number of specific observational consequences, including anomalous multiplicity distributions of the soft pions and a significant enhancement of dilepton production. This idealized DCC formation process is illustrated in Fig. 1.

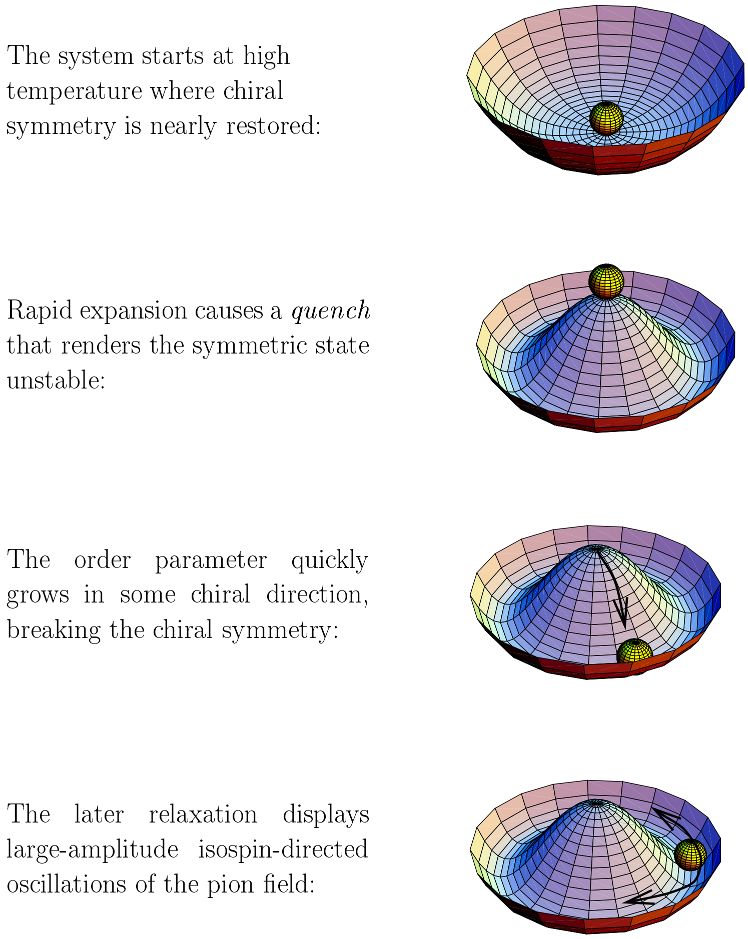

Figure 1. DCC formation.

In the idealized DCC quench scenario, the system is initially so highly agitated that the order parameter is situated at the single minimum of the effective potential near the origin. The system then expands/cools so rapidly that the effective potential quickly reverts to its low-temperature form, in which a nearly degenerate mimimum appears on the surface of the 4-hypersphere with radius f_π, $\sigma^2+\pi^2 \approx f_\pi^2$. Since the early rapid growth of the order parameter is primarily in the radial direction, there is very little vector current generated and the subsequent oscilatory relaxation towards the ground state is therefore well directed in isospace, resulting in a very broad distribution $P(f)$, where $f = n_0/(n_-+n_0+n_+)$ is the neutral fraction of the radiated pions.

1.1. LINEAR SIGMA MODEL

A suitable model framework is presented by the linear σ model, within which a number of investigators have studied various aspects of the DCC dynamics [4-17]. The model describes the degrees of freedom associated with the isoscalar σ field and the isovector $\boldsymbol{\pi}$ field. These are conveniently combined into the (real) $O(4)$ field $\boldsymbol{\phi}$ which has a non-linear equation of motion,

$$\boldsymbol{\phi}(\boldsymbol{r},t) \;=\; (\sigma(\boldsymbol{r},t),\boldsymbol{\pi}(\boldsymbol{r},t)) \;: \qquad \left[\Box+\lambda(\phi^2-v^2)\right]\boldsymbol{\phi} \;=\; H\hat{\sigma}\;. \qquad (1)$$

The three model parameters, λ, v, and H, can be fixed by specifying the pion decay constant f_π and the two meson masses, m_π and m_σ. The vacuum field is aligned with the σ direction, $\boldsymbol{\phi}_{\rm vac}=(f_\pi,\mathbf{0})$, and at low temperatures the agitations of the field represent nearly free σ and π mesons.

2. Phase structure

Instructive insight into the DCC phenomenon can be gained by decomposing the chiral field into a smooth part and the fluctuations around it, $\boldsymbol{\phi}(\boldsymbol{r},t)=\underline{\boldsymbol{\phi}}(t)+\delta\boldsymbol{\phi}(\boldsymbol{r},t)$. The former serves as an *order parameter* characterizing the local vacuum and the latter represent the *quasi-particle* excitations relative to that local vacuum. In the present discussion of matter properties, we shall confine the field to a rectangular box with periodic boundary conditions and the decomposition can then be made in a unique manner (the order parameter $\underline{\boldsymbol{\phi}}$ is then simply the spatial average $\langle\boldsymbol{\phi}\rangle$), but generally it needs to be done locally so $\underline{\boldsymbol{\phi}}$ itself may vary with position.

By taking the spatial average of the full equation of motion (1), it is possible to derive an equation of motion for the order parameter $\underline{\boldsymbol{\phi}}$ [18]. If we subsequently subtract that from (1) and apply a Hartree-type factorization, we obtain corresponding equations for the field fluctuations $\delta\boldsymbol{\phi}$ [12, 19]. The resulting equations of motion are then of mean-field form,

$$\left[\Box+\mu_0^2\right]\underline{\boldsymbol{\phi}}=H\hat{\sigma}\;,\qquad \mu_0^2 \;=\; \lambda[\;\phi_0^2\;+\langle\delta\phi^2\rangle+\;2\langle\delta\phi_{||}^2\rangle-\;v^2]\;, \qquad (2)$$

$$\left[\Box+\mu_{||}^2\right]\delta\phi_{||}=0\;,\qquad \mu_{||}^2 \;=\; \lambda[3\phi_0^2\;+\langle\delta\phi^2\rangle+\;2\langle\delta\phi_{||}^2\rangle-\;v^2]\;, \qquad (3)$$

$$\left[\Box+\mu_{\perp}^2\right]\delta\boldsymbol{\phi}_{\perp}=\mathbf{0}\;,\qquad \mu_{\perp}^2 \;=\; \lambda[\;\phi_0^2\;+\langle\delta\phi^2\rangle+\;2\langle\delta\phi_{\perp}^2\rangle-\;v^2]\;. \qquad (4)$$

Here $\delta\phi_{||}=\delta\boldsymbol{\phi}\circ\hat{\underline{\boldsymbol{\phi}}}$ is the fluctuation along the order parameter and $\delta\boldsymbol{\phi}_\perp$ is the fluctuation perpendicular to $\underline{\boldsymbol{\phi}}$. Furthermore, we have for simplicity ignored the cross terms arising from correlations between field fluctuations in different $O(4)$ directions since they vanish in thermal equilibrium.

To discuss the equilibrium properties, it is natural to consider the partition function associated with the chiral field,

$$\mathcal{Z}_T \;=\; \int \mathcal{D}[\boldsymbol{\psi},\boldsymbol{\phi}]\; \mathrm{e}^{-\frac{\Omega}{T}E[\boldsymbol{\psi},\boldsymbol{\phi}]} \;=\; \int d^4\underline{\boldsymbol{\phi}}\; \mathrm{e}^{-\frac{\Omega}{T}F_T}\;, \tag{5}$$

where $\boldsymbol{\psi}$ denotes the time derivative of the field $\boldsymbol{\phi}$ and plays the role of its conjugate momentum. The statistical weight for finding the system with a specified value of the order parameter $\underline{\boldsymbol{\phi}}$ is given in terms of the associated free energy density which dependes only on the magnitude of the order parameter, ϕ_0, and the angle of disorientation, χ_0 (with $\underline{\sigma} = \phi_0 \cos\chi_0$) [13],

$$\begin{aligned} F_T \;=\;& \tfrac{1}{4}\lambda(\phi_0^2 - v^2)^2 \;-\; H\phi_0\cos\chi_0 \\ +\;& \frac{T}{\Omega}\sum\nolimits'_{\boldsymbol{k}}[\ln(1-\mathrm{e}^{-\epsilon_k^{\parallel}/T}) + 3\ln(1-\mathrm{e}^{-\epsilon_k^{\perp}/T})] \\ -\;& \tfrac{3}{4}\lambda\,[\prec \delta\phi_{\parallel}^2 \succ^2 \;+ 2 \prec \delta\phi_{\parallel}^2 \succ\prec \delta\phi_{\perp}^2 \succ \;+ 5 \prec \delta\phi_{\perp}^2 \succ^2]\;. \end{aligned} \tag{6}$$

The first line is the bare energy associated with a spatially constant field and it represents the local vacuum energy. The second line is the weight of the Bose-Einstein gas of quasiparticles having effective masses $\mu_{\parallel}(T,\phi_0)$ and $\mu_{\perp}(T,\phi_0)$, each term being the partition function of an elementary quasiparticle modes having a particular momentum vector $\boldsymbol{k}$. The last line is the conditional thermal average of the mean-field energy correction.

2.1. PERFECT SYMMETRY

We discuss first the idealized case when chiral symmetry is exact, corresponding to $H = 0$, since this simplified situation has received most theoretical attention [20]. In Fig. 2a is shown the free energy as a function of the magnitude of the order parameter for a range of temperatures, in the macroscopic limit where the volume is large, $\Omega \to \infty$. The equilibrium values of the order parameter can then be obtained by requiring the free energy to have an extremum, $(\partial F_T/\partial\phi_0)_T = 0$. Alternatively, one may be exploit the fact that no dynamical change will occur if the order parameter has its equilibrium value. Since eq. (2) now reads $\ddot{\phi}_0 = -\mu_0^2\phi_0$, this requirement amounts to demanding that $\mu_0^2\phi_0$ vanish. Using the explicit expression (6) for the free energy together with the self-consistent dispersion relations, $\epsilon_{\parallel}^2 = k^2 + \mu_{\parallel}^2$ and $\epsilon_{\perp}^2 = k^2 + \mu_{\perp}^2$, it is elementary to show that

$$\left(\frac{\partial F_T}{\partial \phi_0}\right)_T \;=\; \mu_0^2\;\phi_0\;. \tag{7}$$

This relation ensures that the statistical and dynamical equilibrium criteria are indeed identical, as required by thermodynamic consistency.

For a given temperature, the quasi-particle degrees of freedom can only be in (conditional) thermal equilibrium if the order parameter is sufficiently large to render the square of the effective pion mass positive; otherwise the softest pionic modes have imaginary frequencies and are thus unstable. By $T_0 \approx 130$ MeV, where $T_0^2 = 2v^2$, the region of stability includes all values of the order parameter. Above this temperature, the free energy has a minimum at $\phi_0 = 0$. Moreover, the ground-state minimum occurs at $\phi_0 = v$ and moves steadily inwards as the temperature is increased, until a certain critical temperature is reached, $T_c \approx 190$ MeV. At T_0 a maximum in $F_T(\phi_0)$ appears at $\phi_0 = 0$ and it moves gradually outwards until it joins the outer minimum at T_c; it represents an unstable equilibrium. Since the quasiparticle masses increase with the order parameter, the outer minimum has a more compressed quasiparticle spectrum and thus carries a larger statistical weight. Therefore, it represents the thermodynamcially preferred state at all subcritical temperatures, while the configuration at vanishing ϕ_0 is metastable. Above T_c there is only the symmetric minimum and thus the system prefers chirally configurations. In equilibrium we always have $\mu_0^2 \leq \mu_\perp^2 \leq \mu_\parallel^2$ with the equality signs holding for $\phi_0 = 0$.

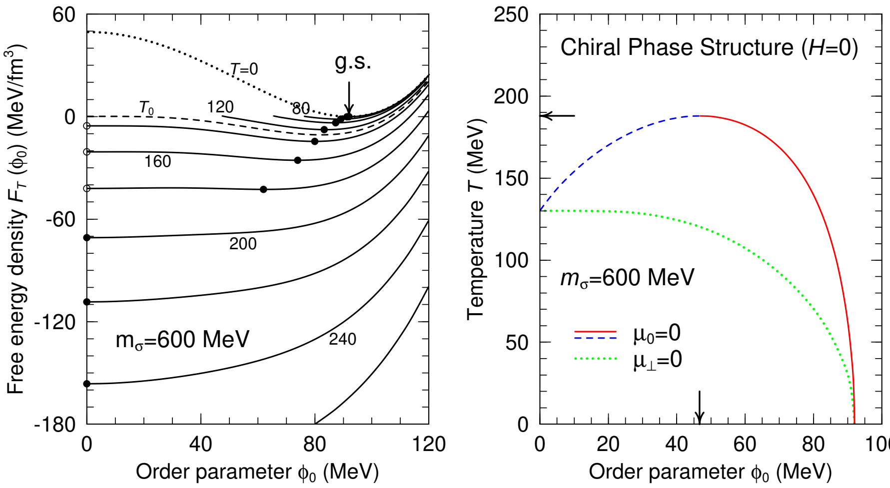

Figure 2. Phase structure.

Part a shows the free energy density F_T as a function of the magnitude of the order parameter, ϕ_0, for a range of temperatures T. For each value of T, the solid dot marks the equilibrium value of ϕ_0, and the open dots mark the metastable equilibria in the intermediate temperature range, $T_0 \leq T \leq T_c$. Part b show the corresponding loci of the stable (solid) and unstable (dashed) equilibria together with the critical boundary (dots) within which the effective field is supercritical and no equilibrium exists.

The structure of the chirally symmeric phase is illustrated in Fig. 2b which shows the thermal path of the equilibrium configuration, characterized by the vanishing of Eq. (7), together with the critical boundary delineated by the condition of a vanishing transverse mass, $\mu_\perp = 0$. The corresponding evolution of the effective quasiparticle masses $\mu_{||}$ and $\mu_\perp$ is shown in Fig. 3a. Because of the general structure of the free energy, the system displays a first-order phase transition at $T = T_c$, with the order parameter abruptly changing from a fairly large finite value to zero. However, the metastable minimum at $\phi_0 = 0$ is very shallow and a finite system would therefore display large fluctuations in ϕ_0. Moreover, even rather small finite values of H will destroy this phase structure, so it has little practical import and merely illustrates what the mean-field treatment would give in the idealized case.

Finally, it is interesting to note the good correspondance of these results with the analytical result expected at low temperatures, as shown in Fig. 3b. The quantitative agreement is very good up to $T \approx 70$ MeV, at which point the analytical result is no longer expected to be adequate. Furthermore, the low-temperature behavior should be independent of m_σ and is indeed found to be so to a high degree.

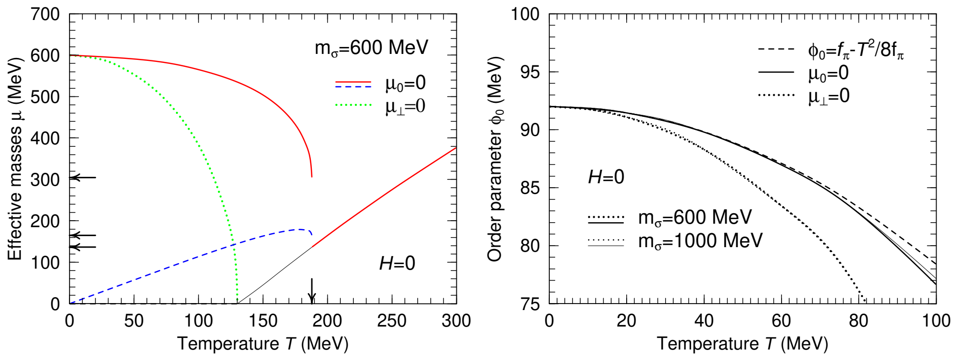

Figure 3. Phase structure.

Part a shows the equilibrium values of the effective masses for the longitudinal (solid) and transverse (dashed) quasiparticle modes, together with the longitudinal mass (dots) along the critical boundary where the transverse mass vanishes; the (degenerate) mass values in the symmetric metastable equilibrium are shown by the thin solid curve. Part b is a magnified view of the behavior of the order parameter at small temperatures (solid), compared with the expected leading-order analytical result [21], $\phi_0 = f_\pi[1 - \frac{1}{8}(T/f_\pi)^2]$ (dash). Two different values of the σ mass are considered and the critical boundary where $\mu_\perp = 0$ is also shown (dots).

2.2. REALISTIC CASE

Since the quark masses are in fact finite, chiral symmetry is only approximate in the real world and the realistic value of the parameter H is much larger than the critical value destroying the special phase structure of the nearly symmetric case discussed above. As a result, there is only one minimum in the free energy for each temperature, and it lies at σ_0 on the positive part of the σ axis. (In addition, at low temperatures there is a maximum on the opposite side near $(-\sigma_0, \mathbf{0})$.) At high temperature, the minimum is located near the origin and chiral symmetry is thus approximately restored. As T is decreased, the accompanying reduction of the field fluctuations causes the free energy to gradually change its appearance, with its minimum moving steadily outwards towards the vacuum value, as shown in Fig. 4*a*. The corresponding temperature dependence of the effective quasi-particle masses is shown in Fig. 4*b*. Starting out at its free value $m_\pi \approx 138$ MeV for T=0, the pion mass grows steadily with T, whereas the σ mass first experiences a significant dip (the minimum occurs at $T_\chi \approx 240$ MeV), before turning upwards and becoming nearly degenerate with the pion mass, as chiral symmetry is approached at high T.

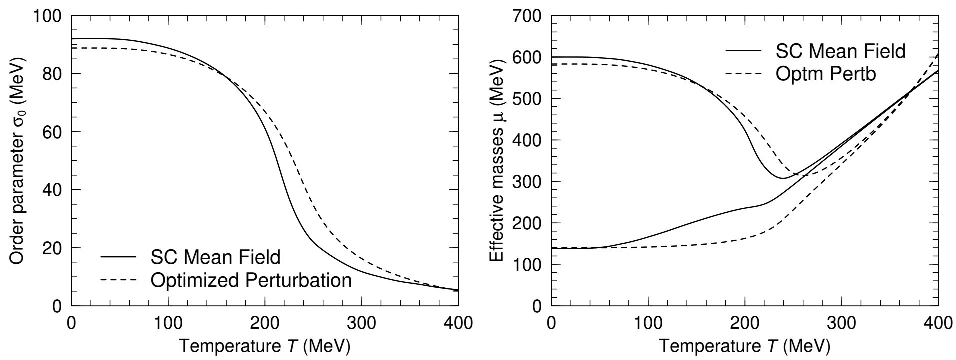

Figure 4. Temperature dependence of order parameter and masses. Part a shows the equilibrium values of the order parameter, σ_0, as a function of the temperature when a realistic strength H of the symmetry-breaking term is employed (solid); part b shows the associated temperature dependence of the effective σ and π masses (solid) [19]. The dashed curves show corresponding results obtained very recently with a quantal treatment employing a novel optimized perturbation method [22, 23]. Since the parameters are not identical, perfect agreement should not be expected. The main difference is thus the steady rise in the pion mass at subcritical temperatures. This shortcoming is likely a consequence of the fact that the mean-field approximation includes only the tadpole diagrams.

3. Dynamics

While the thermal properties provide useful insight, they are of limited direct utility for understanding the non-equilibrium evolution of the chiral degrees of freedom. It is therefore helpful to replace the temperature by the average field fluctuation, $\Delta\phi = \langle\delta\boldsymbol{\phi}\circ\delta\boldsymbol{\phi}\rangle^{1/2}$, since this quantity is meaningful for any individual field configuration $\boldsymbol{\phi}(\boldsymbol{r})$. The resulting display provides a useful "road map" for chiral dynamics and is shown in Fig. 5*a*.

The early violent part of the nuclear collision agitates the system highly and, consequently, nearly restores chiral symmetry. Thus the system is injected into the upper-left part of the Road Map. To emulate the effect of a subsequent scaling expansion, it is instructive to augment the equation of motion (1) with a Rayleigh cooling term, $-(D/t)\partial_t\boldsymbol{\phi}$, where the D is the dimensionality of the expansion [12]. Examples of the resulting dynamical trajectories are displayed in Fig. 5*b*.

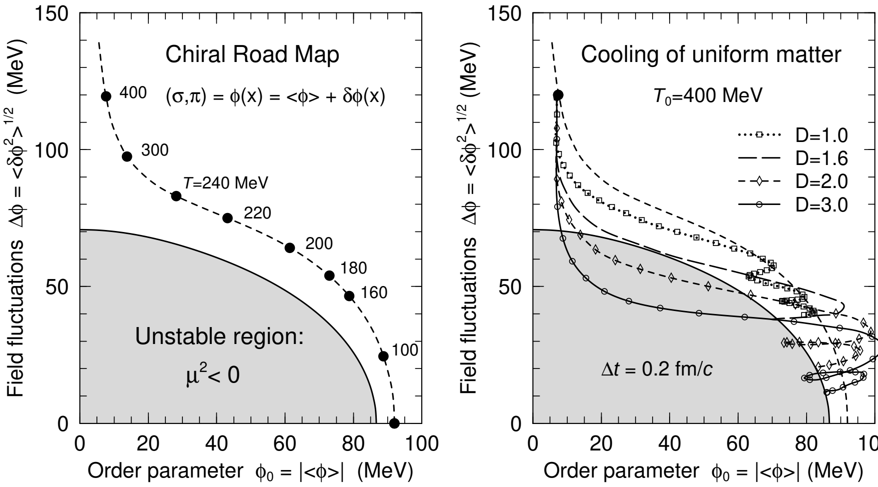

Figure 5. Chiral Road Map.

Part *a* shows the equilibrium path on the "chiral road map" in which the field configuration is projected onto a single point, $\boldsymbol{\phi}(\boldsymbol{r}) \to (\phi_0, \Delta\phi)$. The adiabatic path of equilibrium points (dashed curve), which represents the major "highway", exhibits a gradual cross over from the broken phase at low temperature to the nearly restored phase at high temperature. The shaded area covers the classically forbidden region within which the quasipions are subject to a supercirtical effective field. Part *b* shows the dynamical paths of systems that have been prepared in equilibrium at $T_i = 400$ MeV and then subjected to a Rayleigh cooling with strengths D adjusted to emulate scaling expansions (D=1 emulates a longitudinal Bjorken expansion).

In actual collision scenarios, the expansion is likely to be primarily longitudinal, at least initially, with some transverse expansion gradually appearing in response to the high interior pressure generated. Consistent with earlier findings [10], it appears that a pure longitudinal expansion (D=1) is insufficient to bring the system into the supercritical region, as the dynamical trajectory never strays far from the adiabatic path. On the other hand, an isotropic scaling expansion (D=3) would produce a quench-like scenario by forcing the system well into the unstable region where spontaneous pion pair creation is possible, as already suggested earlier on the basis of a simpler treatment [6]. The resulting scenario of rapid amplification of soft modes is qualitatively similar to the idealized quench [4].

The actual evolution cannot be reliably predicted with the simple linear σ model, as it depends on both the early parton dynamics and couplings to the other degrees of freedom in the system. But it is reasonable to expect the effective expansion to be intermediate between purely longitudinal and fully isotropic, and thus it is hard to know for certain whether the system will in fact experience a quench.

However, irrespectively, it appears that the later part of the relaxation towards the vaccum always proceeds in an oscillatory fashion, with the order parameter executing pronounced quasi-regular motion. This latter feature may give rise to parametric amplification phenomena.

3.1. SIMULATIONS

In order to make more realistic simulations within the linear σ model, it is desirable to recast the field formulation into a more familiar particle-like form, particularly because it is computationally too demanding to treat fields in stongly expanding scenarios due to the boost-induced rapid oscillations in the local field amplitude (only in highly idealized scenarios, such as the pure Bjorken expansion, it is possible to remedy this problem by a suitable coordinate transformation).

Work towards this goal is presently in progress [24]. It invokes the mean-field approximation which appears to provide a quantitatively good approximation for the rapidly expanding dynamical scenarios of interest in the DCC context [13]. A Wigner transformation of the field fluctuations $\delta\phi$ then leads to an approximate Vlasov equation for the quasiparticle phase-space density which may subsequently be represented by a swarm of test-particles, $\{\boldsymbol{r}_n, \boldsymbol{p}_n, \boldsymbol{\chi}_n\}$, for which classical equations of motion are derived, including the dynamics of the quasiparticle chiral spin vectors $\boldsymbol{\chi}_n$ and the self-consistent medium-modified dispersion relation for the quasiparticle energy ω_n. Preliminary tests suggest that this approach may yield a useful framework for simulating DCC dynamics in realistic collision scenarios.

4. Observable consequences

It is useful to consider what observable consequences the DCC phenomenon would have, should the overall dynamics favor its occurrence. Probably the simplest effect is the enhancement of soft pions caused by any excursion into the supercritical region where $\mu_\perp^2 < 0$. Since $\omega_k^2 = k^2 + \mu^2$, the softest pionic modes will then acquire an imaginary frequency and the corresponding field amplitude will grow exponentially, $\pi_k \sim \exp(-i\int\omega_k dt')$. Figure 6*a* shows the shape of the pion power distribution at late times when the cooling has been completed. It is seen how the passage through the supercritical region causes a significant enhancement of soft pions, and the more so the deeper the excursion is. However, because the quasiparticle gas is fairly dilute in phase space, the semi-classical treatment significantly underestimates the effect and an accurate calculation requires quantum field theory.

Since the ultimate relaxation of the order parameter is fairly directed in isospace, the resulting pions tend to be isospin aligned. This key feature suggest examining the neutral pion fraction, $f = n_0/(n_- + n_0 + n_+)$, whose distribution is given by $P(f) = 1/2\sqrt{f}$ if all the pions in each individual event originate from the same fully aligned source. When several independent sources contribute, the effect is eroded and it is therefore essential that the observation focus on just a small part of the system. This effect is illustrated in Fig. 6*b* where the width of $P(f)$ is plotted against the subvolume $\Delta\Omega$ employed when extracting the multiplicities. A suitable experimental zoom may consist of binning the data according to both rapidity y and azimuthal angle ϕ, in addition to the obvious cut on the pion energy.

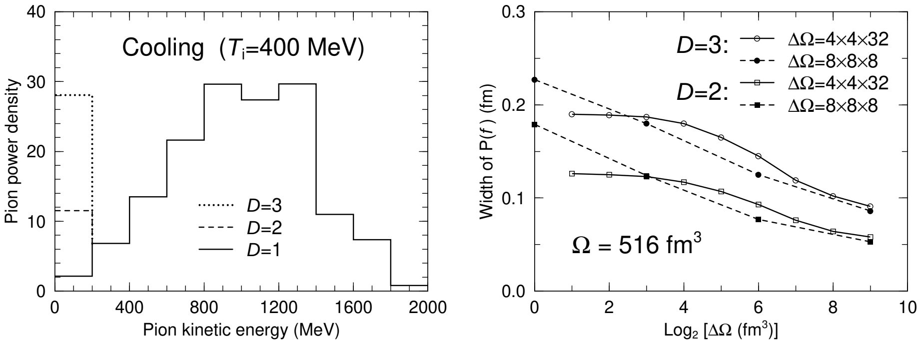

Figure 6. Pion observables

Part *a* shows the final pion power spectrum, after a thermal sample of field configurations has been subjected to Rayleigh cooling with D=1,2,3 [12]. Part *b* shows the width of the extracted neutral fraction distribution $P(f)$ as a function of the volume $\Delta\Omega$ used when extracting the pion multiplicities, for either *cube* (dash) or *rope* (solid) geometries [25].

4.1. ELECTROMAGNETIC SIGNALS

The non-equilibrium DCC evolution following a quench has been found to enhance the production of dileptons [26] and photons [27]. In particular, more elaborate (but still idealized) calculations suggest that the interaction of the oscillating order parameter with the surrounding thermal pions may enhance the yield of dileptons with invariant masses near and below $\frac{1}{2}m_\sigma$ by more than an order of magnitude [28]. Certainly, more realistic scenarios need to be considered. Moreover, it still needs to be determined if such a signal could be experimentally visible through the considerable background.

5. Outlook

High-energy collisions of nuclei makes it possible to explore new phases of matter and the associated transitions, in particular the deconfinement transition and of themthe restoration of chiral symmetry, both fundamental features of quantum chromodynamics.

The present discussion has concentrated on the chiral degrees of freedom in strongly interacting matter, as described within the linear σ model in the semi-classical treatment. In the well-studied but unrealistic case of perfect chiral symmetry, the mean-field treatment produces a first-order transition. However, when the finite quark masses are taken into account, this delicate structure is replaced by a smooth crossover from the low-temperature broken phase toward approximate chiral symmetry at high temperatures. Nevertheless, in all scenarios, there is an extended phase region in which the field is supercritical so that spontaneous pion pair creation is possible. If the collision dynamics leads to a sufficiently rapid expansion then the resulting quench brings the system into the unstable region and a strong enhancement of soft pions occurs. Even if a quench is not produced, the oscillatory behavior of the order parameter at late times is likely to cause parametric amplification of both the hadronic and the electromagnetic signals.

The search for this novel phenomenon in high-energy collisions should probably be multipronged, since any individual signal may be neither very strong nor even unique. For example, the expected broadening of the neutral fraction distribution $P(f)$ can also be accomplished by a simple reduction in the freezeout temperature and advanced methods, such as wavelet analysis [25, 29], may therefore be required to extract the non-equilibrium component. It is fortunate that although the occurrence of disoriented chiral condensates is inherently a strong-interaction phenomenon, there are also specific electromagnetic signals. One may then hope that the combination of the different types of observable may make it practically feasible to experimentally explore the dynamics of the chiral phase transition.

It is a pleasure to acknowledge helpful and illuminating discussions with many colleagues, especially Tetsuo Hatsuda, Volker Koch, Jochem Wambach, and Wolfram Weise.

References

1. K. Rajagopal, in *Quark-Gluon Plasma 2*, ed. R. Hwa, World Scientific (1995)
2. J.-P. Blaizot and A. Krzywicki, Acta Phys. Polon. B27 (1996) 1687
3. J.D. Bjorken, Acta Phys. Polon. B28 (1997) 2773
4. K. Rajagopal and F. Wilczek, Nucl. Phys. B404 (1993) 577
5. S. Gavin, A. Gocksch, and R.D. Pisarski, Phys. Rev. Lett. 72 (1994) 2143
6. S. Gavin and B. Müller, Phys. Lett. B329 (1994) 486
7. J.-P. Blaizot and A. Krzywicki, Phys. Rev. D50 (1994) 442
8. Z. Huang and X.-N. Wang, Phys. Rev. D49 (1994) 4335
9. F. Cooper, Y. Kluger, E. Mottola, and J.P. Paz, Phys. Rev. D51 (1995) 2377
10. M. Asakawa, Z. Huang, and X.-N. Wang, Phys. Rev. Lett. 74 (1995) 3126
11. L.P. Csernai and I.N. Mishustin, Phys. Rev. Lett. 74 (1995) 5005
12. J. Randrup, Phys. Rev. Lett. 77 (1996) 1226
13. J. Randrup, Nucl. Phys. A616 (1997) 531
14. T.S. Biro, D. Molnár, Z. Feng, and L.P. Csernai, Phys. Rev. D55 (1997) 6900
15. T.S. Biro and C. Greiner, Phys. Rev. Lett. 79 (1997) 3138
16. G. Amelino-Camelia, J.D. Bjorken, and S.E. Larsson Phys. Rev. D56 (1997) 6942
17. A. Abada and M.C. Birse, Phys. Rev. D57 (1998) 292
18. G. Baym and G. Grinstein, Phys. Rev. D15 (1977) 2897
19. J. Randrup, Phys. Rev. D55 (1997) 1188
20. The literature is abundant with studies of models with $O(N)$ symmetry and the following limited selection of references may help to guide interested readers: S. Coleman and E. Weinberg, Phys. Rev. D7 (1973) 1888; L. Dolan and R. Jackiw, Phys. Rev. D9 (1974) 3320; G. Baym and G. Grinstein, Phys. Rev. D15 (1977) 2897; W.A. Bardeen and M. Moshe, Phys. Rev. D34 (1986) 1229; R. Allés and R. Tarrach, Phys. Rev. D33 (1986) 1718; N. Tetradis and C. Wetterlich, Nucl. Phys. B398 (1993) 659; W. Buchmüller, T. Helbig, and D. Walliser, Nucl. Phys. B407 (1993) 387
21. P. Gerber and H. Leutwyler, Nucl. Phys. B321 (1989) 387
22. S. Chiku and T. Hatsuda, Phys. Rev. D57 (1998) R6
23. S. Chiku and T. Hatsuda, *hep-ph/9803226*: Phys. Rev. D (1998) in press
24. J. Randrup, LBL-41202: Phys. Lett. B (1998) in press
25. J. Randrup and R.L. Thews, Phys. Rev. D56 (1997) 6392
26. Z. Huang and X.N. Wang, Phys. Lett. B383 (1996) 457
27. D. Boyanovsky, H.J. de Vega, R. Holman, S.P. Kumar, Phys. Rev. D56 (1997) 5233
28. Y. Kluger, V. Koch, J. Randrup, and X.N. Wang, Phys. Rev. C57 (1998) 280
29. Z. Huang, I. Sarcevic, R. Thews, and X.N. Wang, Phys. Rev. D54 (1996) 750